Tracking Temperature-Dependent Relaxation Times of Ferritin Nanomagnets with a Wideband Quantum Spectrometer

Eike Schäfer-Nolte,[1,2] Lukas Schlipf,[1,2] Markus Ternes,[1,*] Friedemann Reinhard,[2] Klaus Kern,[1,3] and Jörg Wrachtrup[2,1]
[1]*Max-Planck Institute for Solid State Research, 70569 Stuttgart, Germany*
[2]*3rd Institute of Physics and Research Center SCoPE, University Stuttgart, 70569 Stuttgart, Germany*
[3]*Institut de Physique de la Matière Condensée, École Polytechnique Fédérale de Lausanne, 1015 Lausanne, Switzerland*
(Received 2 June 2014; published 20 November 2014)

We demonstrate the tracking of the spin dynamics of ensemble and individual magnetic ferritin proteins from cryogenic up to room temperature using the nitrogen-vacancy color center in diamond as a magnetic sensor. We employ different detection protocols to probe the influence of the ferritin nanomagnets on the longitudinal and transverse relaxation of the nitrogen-vacancy center, which enables magnetic sensing over a wide frequency range from Hz to GHz. The temperature dependence of the observed spectral features can be well understood by the thermally induced magnetization reversals of the ferritin and enables the determination of the anisotropy barrier of single ferritin molecules.

DOI: 10.1103/PhysRevLett.113.217204 PACS numbers: 75.75.Jn, 76.30.Mi

The study of magnetic fluctuations—time-dependent deviations of a magnetic system from equilibrium—is of high intrinsic interest and provides a powerful tool to gain insight into magnetic coupling mechanisms. For example, magnetic fluctuations provide important information on the physics of highly correlated electron systems [1,2]. Experimentally, however, access to fluctuations is frequently challenging, for two reasons: Firstly, fluctuations can extend over an excessively large range of frequencies. Secondly, many relevant magnetic systems are small entities with dimensions in the nanometer range, such as single molecules, clusters, or magnetic domains. Hence, the study of magnetic fluctuations requires a measurement technique featuring simultaneously nanoscale resolution and a wide frequency bandwidth.

Widely used methods to study ensembles of magnetic nanosystems are SQUID magnetometry [3,4], Mössbauer spectroscopy [5], electron spin resonance [6], neutron scattering [7], or x-ray magnetic circular dichroism [8]. Furthermore, individual magnetic nano-objects have been investigated by scanning probe microscopy [9,10], micro SQUIDs [11,12] or scanning x-ray microscopy [13]. In general, these techniques have a limited detection bandwidth, such that the experimental observation of magnetic fluctuations in a wide frequency range relies on stitched measurements combining complementary techniques in different frequency domains.

Here we show that the nitrogen-vacancy (NV) center in diamond employed as a magnetic field sensor [14,15] simultaneously provides access to both nanoscale objects and a frequency bandwidth spanning 10 orders of magnitude. By employing different interrogation techniques we monitor thermal magnetization reversals of single biological nanomagnets from cryogenic to room temperature where these fluctuations accelerate from the sub-Hz to the GHz range.

We study ferritin protein complexes adsorbed onto a diamond surface [Fig. 1(a)]. Besides its physiological importance for the iron storage in mammals [16], ferritin attracted much attention as a model system for nanoparticle magnetism [5,17,18]. Each of these proteins encloses a cluster of up to 4500 Fe atoms whose net magnetic moment exhibits strong thermally activated fluctuations. We detect the magnetic stray field of these clusters with NV defect centers embedded 5–10 nm below the diamond surface. This center enables the precise determination of the local magnetic field via the Zeeman shift of its spin sublevels, which can be measured by optically detected magnetic resonance (ODMR) techniques. Because of its atomic size, an individual NV center can be placed as a sensor spin in nanometer proximity to the sample [15,19], allowing for coupling to only a single ferritin complex. Moreover, it can sense magnetic field fluctuations on various frequency scales from the sub-Hz [20] over the kHz to MHz

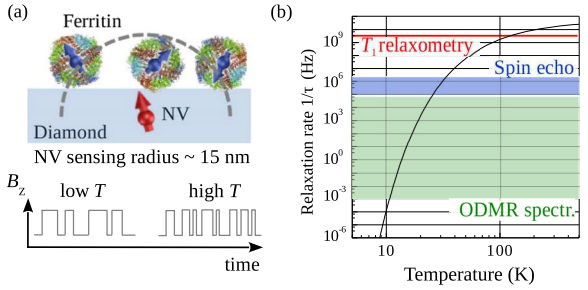

FIG. 1 (color online). (a) Ferritin molecules adsorbed to the diamond surface couple to shallow implanted NV centers. The magnetization reversals of the ferritin generate magnetic telegraph noise with a temperature-dependent fluctuation rate. (b) Ferritin relaxation rate as a function of temperature for $E_a = 29$ meV. The sensitivity ranges of different detection protocols for NV magnetometry are indicated.

[21,22] to the GHz range [23], depending on the spectroscopy protocol employed. As a notable extension of previous studies, here we demonstrate nanosensing in a variable temperature setup between 5 and 300 K in ultrahigh vacuum [24].

Over this temperature range, magnetic fluctuations of ferritin cores exhibit a rich variety of dynamic phenomena like superparamagnetism [25], superantiferromagnetism [4], and macroscopic quantum tunneling [3]. The Fe atoms in the biomineral core are stored in the form of a hydrous ferric oxide-phosphate mineral similar in structure to ferrihydrate [17]. At lower temperatures the Fe^{3+} spins are antiferromagnetically coupled with a Neél temperature estimated to be between 240 [17] and 500 K [4]. In the antiferromagnetic phase, the ferritin core possesses a net magnetic moment on the order of $300\mu_B$ due to an imperfect compensation of the Fe^{3+} spins on the two sublattices [5,26]. The core is generally considered as single magnetic domain with uniaxial anisotropy; therefore, the magnetic moment fluctuates thermally activated between the two directions along the easy axis of magnetization with a temperature-dependent rate. The dynamics of these stochastic magnetization reversals is characterized by the spin lifetime

$$\tau(T, E_a) = \tau_0 \exp(E_a/k_B T), \tag{1}$$

with the inverse attempt frequency $\tau_0 \approx 2 \times 10^{-11}$ s [7] and the anisotropy barrier E_a. This anisotropy barrier is dominated by the magnetocrystalline energy and scales thus with the volume of the core. Additional contributions arise from surface effects, strain, and the particle shape [5]. The magnetization reversals of an individual molecule with the temperature-dependent relaxation rate $1/\tau$ [Fig. 1(b)] generates magnetic field fluctuations resembling random telegraph noise. The normalized spectral density of this spin noise is calculated to [23]

$$S(\omega, T, E_a) = \frac{2}{\pi} \frac{\tau(T, E_a)}{1 + \tau(T, E_a)^2 \omega^2}. \tag{2}$$

With lower temperatures the cutoff frequency of $S(\omega, T, E_a)$ decreases, while the low-frequency amplitude increases (Fig. 2). To account for the spread of E_a in the measured ferritin ensembles, we assume a log-normal distribution function [27].

Our method to detect these fluctuations is based on changes in the longitudinal (T_1) or transverse (T_2, T_2^*) [28] spin relaxation time of the NV center in response to the ferritin spin noise. The relaxation rate of the NV center can be written in general as

$$\frac{1}{T_i} = \left(\frac{1}{T_i}\right)_{\text{int}} + \int \gamma^2 \langle B^2 \rangle S(\omega, T, E_a) F_i(\omega) d\omega, \tag{3}$$

where $(T_i^{-1})_{\text{int}}$ accounts for intrinsic relaxation mechanisms, γ is the gyromagnetic ratio of the NV center, and

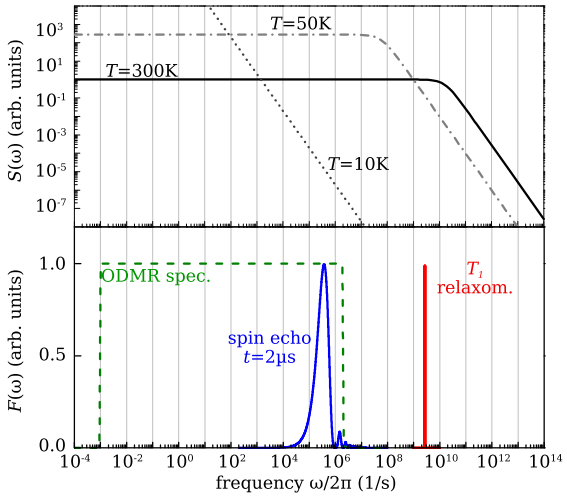

FIG. 2 (color online). Spectral density $S(\omega)$ of the ferritin spin noise at different temperatures for an anisotropy barrier of $E_a = 25$ meV. The filter functions $F(\omega)$ of T_1 relaxometry, two-pulse spin echo spectroscopy, and an empirical approximation for ODMR spectroscopy are depicted below.

$\sqrt{\langle B^2 \rangle}$ is the effective magnetic field at the NV position generated by the magnetic ferritin core, corresponding to the distance-dependent dipolar coupling strength. In this equation the spectral response function $F_i(\omega)$ depends on the employed sensing protocol. To access different frequency ranges, we probe the relaxation of the NV center by the inversion recovery protocol [29], two-pulse spin echo spectroscopy [30], and one-pulse ODMR spectroscopy [20]. The corresponding response functions and spectral sensitivity ranges are summarized in Table I and Fig. 2. We assumed as an empirical approximation a constant sensitivity in a frequency window limited by the acquisition time per spectrum $t_{\text{acq}} = 10^3$ s and the length of the microwave pulse $t_\pi = 500$ ns. A constant external magnetic field on the order of 6 mT was applied with the direction chosen such that the resonance transitions for the four NV orientations are spectrally separated.

With decreasing temperature the ferritin noise spectrum is subsequently shifted through these distinct sensitivity windows, which we verify by measurements on an ensemble of ferritin molecules (Fig. 3). Without adsorbed ferritin we measure $T_1 = 0.67 \pm 0.15$ ms at $T = 300$ K, which increases to > 2.5 ms at low temperature, i. e., above the longest decay time detectable in our setup. Upon the adsorption of ferritin molecules, the T_1 time at room temperature is reduced by approximately a factor of 5, which has been previously observed for bulk diamonds [31] and diamond nanocrystals [32]. The ferritin-induced reduction in T_1 vanishes at low temperatures, since the cutoff frequency of the ferritin noise spectrum shifts below the NV transition frequency. In the low-temperature regime ($k_B T \ll E_a$) the ferritin magnetization is static on the time scale of the measurement, since magnetization reversals

TABLE I. Filter functions $F(\omega)$ and corresponding frequency ranges for the employed detection protocols. $\Gamma = 1/T_2^*$, NV dephasing rate; ω_L, NV transition frequency; t, free evolution time; c, normalization constant; t_{acq}, acquisition time; t_π, microwave pulse length.

Technique	Filter function $F_i(\omega)$	Frequency range	Reference
T_1 relaxometry	$(1/\pi)\Gamma/[\Gamma^2 + (\omega - \omega_L)^2]$	~3 GHz	[29]
Spin echo	$(1/t)\lvert\sin^2(\omega t/4)/(\omega/4)\rvert^2$	0.1–1 MHz	[30]
ODMR spectroscopy	$\begin{cases} 1/c, & 2\pi/t_{\mathrm{acq}} < \omega < 2\pi/t_\pi \\ 0, & \text{else} \end{cases}$	10^{-3}–10^6 Hz	[20]

over the energy barrier are suppressed. The data show thus a strong increase in T_1 below the blocking temperature of $T_B \approx 50$ K, which we can well describe within our model using $\bar{E}_a = (15 \pm 5)$ meV and $\sqrt{\langle B^2 \rangle} = (0.79 \pm 0.15)$ mT. We note that NV centers close to nonadsorbed surfaces show a drastically different temperature behavior with T_1 times of up to 100 ms at 5 K [33].

To probe the temperature dependence of the ferritin magnetization dynamics in the range 0.1–1 MHz, we employ spin echo spectroscopy. The coherence time T_2 time is rather unaffected by the ferritin spin noise at 300 K, due to the low noise amplitude in the probed frequency range [Fig. 3(b)]. This changes at low temperatures; as the cutoff frequency of the ferritin noise spectrum decreases, the noise amplitude in the probed frequency range initially increases. The ferritin contribution to the relaxation rate becomes dominant for $T \lesssim 80$ K, leading to a reduction of T_2. At $T \lesssim 35$ K, the cutoff frequency of the ferritin noise spectrum shifts below the detection window of the spin echo sequence, resulting in a recovery of the T_2 time. The minimum in T_2 at roughly 35 K corresponds to the blocking temperature for the probed frequency range. The reference measurement acquired without adsorbed ferritin shows only a modest increase of T_2 with lower temperature, which might be related to temperature-dependent intrinsic relaxation processes. We reach an overall good agreement when fitting the data with the above-described model, yielding $\bar{E}_a = (25 \pm 5)$ meV and $\sqrt{\langle B^2 \rangle} = (0.39 \pm 0.15)$ mT.

The deviation of $\bar{E}_a$ and $\sqrt{\langle B^2 \rangle}$ between the T_1 and T_2 measurement can be rationalized by the simplicity of the employed model and the fact that different samples were used. In particular, the difference in the coupling strength is presumably due to different thicknesses of the molecular layers. We note that the obtained parameters are rather unaffected by the exact temperature dependence of the intrinsic NV relaxation rate assumed in the model. Overall, the results correspond well to reported average anisotropy barriers in ferritin of ~28 meV determined by Mössbauer spectroscopy and magnetization measurements [27,34].

We obtain further insight into the ferritin spin dynamics especially at low frequencies by ODMR spectroscopy [Fig. 3(c)]. We detect at 5 K an increase of the resonance linewidth by ~5 MHz compared to data measured at 77 K, which can be interpreted in the framework of the ODMR filter function: At $T \geq 77$ K, the fluctuations of the magnetic moments are fast compared to the inverse microwave pulse length (500 ns), such that only the average magnetization of the molecular ensemble is detected (motional narrowing regime). At 5 K, the spin dynamics of most molecules is blocked, i.e., their magnetization is static over the measurement time (~10^3 s), and thus the local magnetic field differs for each NV center depending on the size and the orientation of the nearby molecules

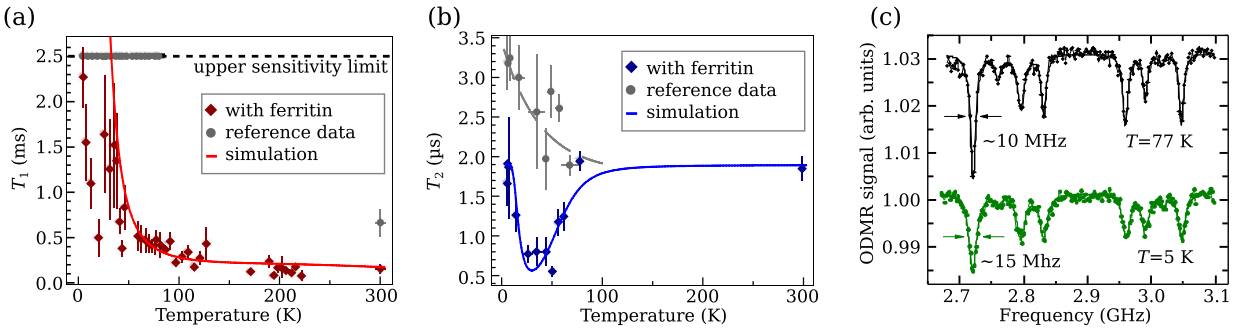

FIG. 3 (color online). Measurements on NV ensembles interacting with ferritin molecules. (a) Longitudinal relaxation time T_1 (diamonds) and simulation using $\bar{E}_a = (15 \pm 5)$ meV and $\sqrt{\langle B^2 \rangle} = (0.79 \pm 0.15)$ mT (full line). The longest detectable decay time of 2.5 ms is indicated as upper sensitivity limit by the dashed line. (b) Spin coherence time T_2 (diamonds) and simulation using $\bar{E}_a = (25 \pm 5)$ meV and $\sqrt{\langle B^2 \rangle} = (0.39 \pm 0.15)$ mT (full line). Reference data without ferritin in (a) and (b) are shown as circles. (c) ODMR spectra acquired at 5 and 77 K.

(inhomogeneous broadening [6]). The low-temperature linewidth of ~15 MHz corresponds to an effective internal field in the NV center ensemble of ~0.53 mT, which is comparable to the coupling strength $\sqrt{\langle B^2 \rangle}$ estimated from the T_1 and T_2 measurements. This value is consistent with the expected stray field of ferritin molecules ($\mu \approx 300 \mu_B$) on the diamond surface.

The obtained blocking temperatures can be compared to values reported for horse-spleen ferritin using other detection techniques; susceptibility measurements (characteristic measurement time $\tau_m \sim 10^{-3}$–10^{2} s) yield blocking temperatures in the range 5–20 K [3,5,26,34], Mössbauer spectroscopy ($\tau_m \sim 10^{-8}$ s) 30–50 K [5,17,25], and electron spin resonance ($\tau_m \sim 10^{-10}$ s) ~100 K [6]. Our findings using NV magnetometry are thus consistent with previously reported results. We point out that NV magnetometry can cover a significantly wider frequency range than the abovementioned techniques. By using other detection protocols or varying the external magnetic field, a further extension of the sensitivity range or an enhancement of the spectral resolution can be achieved [35,36].

An important advantage of the NV sensor is the very high sensitivity with the potential for the investigation of single molecules [15,19]. To utilize this capability we used a diamond substrate with low NV concentration enabling us to optically address and readout individual centers. Ferritin was deposited with reduced coverage such that isolated molecules are obtained, which was confirmed by atomic force microscopy. The average distance between molecules and NV centers was around 20 nm. Thus, only a few molecules are expected to interact with each NV. We studied the same NV centers (~35 in total) before and after ferritin deposition and found for roughly 50% a pronounced reduction of T_1 at room temperature. These centers interacting with only one or a few molecules were investigated at variable temperature.

Figure 4(a) shows the coherence time T_2 for a representative single NV center revealing minima at 47 and 62 K. Measurements on other NV centers yield similar curves with one or multiple minima with a rather small width. The dips in T_2 fall in the same temperature range as the broad feature observed in the ensemble measurements [Fig. 3(b)]. To model the response of the NV center to a single molecule, we used $S(\omega)$ without ensemble broadening and found a good agreement to the observed minimum in T_2 at $T = 47$ K (62 K) using $E_a = 45 \pm 5$ meV (60 ± 5 meV) and $\sqrt{\langle B^2 \rangle} = 54 \pm 10\,\mu$T ($36 \pm 8\ \mu$T) [Fig. 4(b)]. The width of the calculated minimum is on the order of 10 K, which corresponds well to the sharp features observed in the experiment. These findings support the interpretation that the observed minima are fingerprints of individual molecules with different blocking temperatures in the vicinity of the NV center. This technique thus enables the determination of anisotropy barriers on the single molecule level.

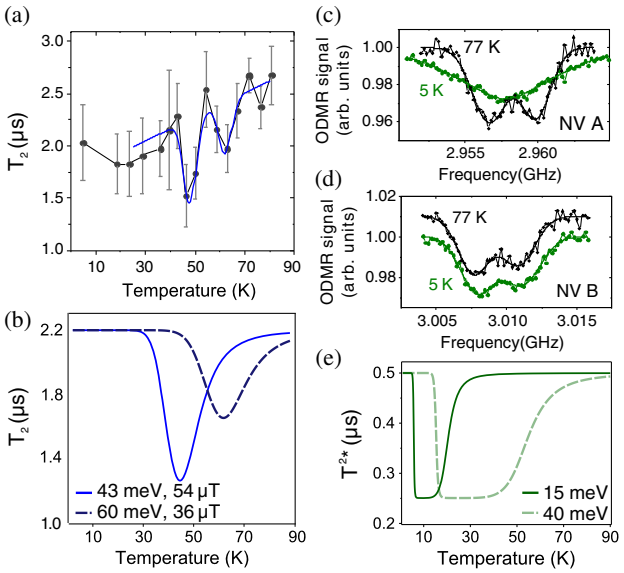

FIG. 4 (color online). (a) Temperature-dependent T_2 of a single NV center interacting with isolated molecules. The full line marks the two minima. (b) Calculated temperature dependence of T_2 for a NV center coupling to single molecules with different E_a and $\sqrt{\langle B^2 \rangle}$. (c),(d) Representative ODMR spectra of single NV centers. Low-temperature line broadening as shown in (a) was observed for ~20% of the investigated NV centers. (e) Calculated temperature dependence of T_2^* for a NV center coupling to ferritin molecules with different anisotropy barrier and a coupling of $\sqrt{\langle B^2 \rangle} = 180\ \mu$T.

The low-temperature resonance linewidth in the ODMR spectra of single NV centers depends on the anisotropy barrier of the nearby molecules. We observe a broadening at 5 K for roughly 20% of the investigated NV centers [Fig. 4(c)], which we attribute to the magnetic fluctuations of molecules with rather low anisotropy energy such that $T_B < 5$ K. In contrast, most NV centers show similar line shapes at 5 and 77 K [Fig. 4(d)], suggesting that nearby molecules are blocked at 5 K. The calculated temperature dependence of the NV decoherence time T_2^* (proportional to the inverse linewidth) shown in Fig. 4(e) indicates that the low-temperature line broadening is related to molecules with $E_a < 15$ meV, which is consistent with the expected spread of anisotropy energies in the sample [27].

The static magnetization of the blocked ferritin molecules is expected to result in a random shift of the transition frequency between 5 and 77 K. Experimentally we find this shift to be ~1 MHz, corresponding to an effective field of ~36 μT, for all NV centers studied, which is significantly smaller then the line broadening of ~5 MHz (~180 μT) observed for the unblocked molecules [Fig. 4(c)]. This deviation in the coupling strength might be related to the existence of a second magnetic phase located at the particle surface [6,37], which aligns antiparallel to the interior of the core at low temperature and thus reduces the net magnetic moment.

In conclusion, we demonstrated the detection of the temperature-dependent relaxation dynamics of ferritin molecules by employing NV magnetometry. The main advantages of this approach are the wide frequency range that can be covered and the high sensitivity enabling single molecule experiments. While in the single NV center experiments demonstrated here the number of detected ferritin molecules could only be estimated, future experiments using NV spin sensors in a scanning probe architecture [24,38,39] will facilitate single molecule investigations with enhanced control and precision. For example, this method could be used to address the validity of Eq. (1) and to determine the preexponential factor, which is still under debate in the literature [7]. Because of its high sensitivity and its intrinsic spatial resolution, the technique can also be applied to investigate systems with smaller magnetic moment, such as molecular magnets, radicals, or, ultimately, nuclear spins.

F. R. and J. W. acknowledge financial support by the EU (Squtec, Diadems), Darpa (Quasar), BMBF (CHIST-ERA), and contract research of the Baden-Württemberg foundation.

*m.ternes@fkf.mpg.de

[1] P. A. Lee, N. Nagaosa, and X. G. Wen, Rev. Mod. Phys. **78**, 17 (2006).
[2] A. C. Hewson, *The Kondo Problem to Heavy Fermions* (Cambridge University Press, Cambridge, England, 1997).
[3] S. Gider, D. D. Awschalom, T. Douglas, S. Mann, and M. Chaparala, Science **268**, 77 (1995).
[4] C. Gilles, P. Bonville, H. Rakoto, J. M. Broto, K. K. W. Wong, and S. Mann, J. Magn. Magn. Mater. **241**, 430 (2002).
[5] G. C. Papaefthymiou, Biochim. Biophys. Acta **1800**, 886 (2010).
[6] E. Wajnberg, L. J. El-Jaick, M. P. Linhares, and D. M. S. Esquivel, J. Magn. Reson. **153**, 69 (2001).
[7] S. Mørup, D. E. Madsen, C. Frandsen, C. R. H. Bahl, and M. F. Hansen, J. Phys. Condens. Matter **19**, 213202 (2007).
[8] P. Gambardella, S. Rusponi, M. Veronese, S. S. Dhesi, C. Grazioli, A. Dallmayer, I. Cabria, R. Zeller, P. H. Dederichs, K. Kern, C. Carbone, and H. Brune, Science **300**, 1130 (2003).
[9] S. Loth, S. Baumann, C. P. Lutz, D. M. Eigler, and A. J. Heinrich, Science **335**, 196 (2012).
[10] A. A. Khajetoorians, B. Baxevanis, C. Hübner, T. Schlenk, S. Krause, T. O. Wehling, S. Lounis, A. Lichtenstein, D. Pfannkuche, J. Wiebe, and R. Wiesendanger, Science **339**, 55 (2013).
[11] W. Wernsdorfer, Nat. Mater. **6**, 174 (2007).
[12] P. F. Vohralik and S. K. H. Lam, Supercond. Sci. Technol. **22**, 064007 (2009).
[13] A. Balan, P. M. Derlet, A. F. Rodriguez, J. Bansmann, R. Yanes, U. Nowak, A. Kleibert, and F. Nolting, Phys. Rev. Lett. **112**, 107201 (2014).
[14] A. Gruber, Dräbenstedt, C. Tietz, L. Fleury, J. Wrachtrup, and Borczyskowski, Science **276**, 2012 (1997).
[15] J. M. Taylor, P. Cappellaro, L. Childress, L. Jiang, D. Budker, P. R. Hemmer, A. Yacoby, R. Walsworth, and M. D. Lukin, Nat. Phys. **4**, 810 (2008).
[16] M. C. Linder, Nutrients **5**, 4022 (2013).
[17] E. R. Bauminger and I. Nowik, Hyperfine Interact. **50**, 489 (1989).
[18] J. H. Cole and L. C. L. Hollenberg, Nanotechnology **20**, 495401 (2009).
[19] C. L. Degen, Nat. Nanotechnol. **3**, 643 (2008).
[20] A. Dréau, M. Lesik, L. Rondin, P. Spinicelli, O. Arcizet, J.-F. Roch, and V. Jacques, Phys. Rev. B **84**, 195204 (2011).
[21] T. Staudacher, F. Shi, S. Pezzagna, J. Meijer, J. Du, C. A. Meriles, F. Reinhard, and J. Wrachtrup, Science **339**, 561 (2013).
[22] H. J. Mamin, M. Kim, M. H. Sherwood, C. T. Rettner, K. Ohno, D. D. Awschalom, and D. Rugar, Science **339**, 557 (2013).
[23] S. Steinert, F. Ziem, L. T. Hall, A. Zappe, M. Schweikert, N. Götz, A. Aird, G. Balasubramanian, L. Hollenberg, and J. Wrachtrup, Nat. Commun. **4**, 1607 (2013).
[24] E. Schaefer-Nolte, F. Reinhard, M. Ternes, J. Wrachtrup, and K. Kern, Rev. Sci. Instrum. **85**, 013701 (2014).
[25] R. B. Frankel, G. C. Papaefthymiou, and G. D. Watt, Hyperfine Interact. **66**, 71 (1991).
[26] J. G. E. Harris, J. E. Grimaldi, D. D. Awschalom, A. Chiolero, and D. Loss, Phys. Rev. B **60**, 3453 (1999).
[27] D. E. Madsen, M. F. Hansen, J. Bendix, and S. Mørup, Nanotechnology **19**, 315712 (2008).
[28] T_2^* is the spin decoherence time affected mainly by low-frequency noise compared to $T_2 > T_2^*$ which is only sensitive to noise in the detection window at higher frequency.
[29] A. Jarmola, V. M. Acosta, K. Jensen, S. Chemerisov, and D. Budker, Phys. Rev. Lett. **108**, 197601 (2012).
[30] A. Laraoui, J. S. Hodges, and C. A. Meriles, Appl. Phys. Lett. **97**, 143104 (2010).
[31] F. Ziem, N. S. Götz, A. Zappe, S. Steinert, and J. Wrachtrup, Nano Lett. **13**, 4093 (2013).
[32] A. Ermakova, G. Pramanik, J.-M. Cai, G. Algara-Siller, U. Kaiser, T. Weil, Y.-K. Tzeng, H.-C. Chang, L. P. McGuinness, M. B. Plenio, B. Naydenov, and F. Jelezko, Nano Lett. **13**, 3305 (2013).
[33] S. A. Momenzadeh, R. J. Stöhr, F. F. de Oliveira, A. Brunner, A. Denisenko, S. Yang, F. Reinhard, and J. Wrachtrup, arXiv:1409.0027.
[34] S. H. Kilcoyne and R. Cywinski, J. Magn. Magn. Mater. **144**, 1466 (1995).
[35] V. M. Acosta, E. Bauch, A. Jarmola, L. J. Zipp, M. P. Ledbetter, and D. Budker, Appl. Phys. Lett. **97**, 174104 (2010).
[36] C. S. Shin, C. E. Avalos, M. C. Butler, D. R. Trease, S. J. Seltzer, J. P. Mustonen, D. J. Kennedy, V. M. Acosta, D. Budker, A. Pines, and V. S. Bajaj, J. Appl. Phys. **112**, 124519 (2012).
[37] R. A. Brooks, J. Vymazal, D. Goldfarb, J. W. M. Bulte, and P. Aisen, Magn. Reson. Med. **40**, 227 (1998).
[38] P. Maletinsky, S. Hong, M. S. Grinolds, B. Hausmann, M. D. Lukin, R. Walsworth, M. Loncar, and A. Yacoby, Nat. Nanotechnol. **7**, 320 (2012).
[39] L. Rondin, J.-P. Tetienne, P. Spinicelli, C. Dal Savio, K. Karrai, G. Dantelle, A. Thiaville, S. Rohart, J.-F. Roch, and V. Jacques, Appl. Phys. Lett. **100**, 153118 (2012).